

ENABLING REPEAT-PASS INTERFEROMETRY FROM LOW VENUS ORBIT

Mark S Wallace^{*}, Theodore H. Sweetser[†], Robert J. Haw[‡], Eunice Lau[§], and Scott Hensley^{**}

Repeat-pass interferometry is a powerful technique for determining changes in topography by flying a radar over the terrain two or more times. These overflights must be very close to each other in space. To design and maintain a low Venus orbit that enables this requires the consideration of drag, non-spherical gravity effects, and solar tides. Once the orbit is designed, the spacecraft must be navigated. To do so requires the use of radar-based terrain-relative navigation in addition to the traditional radiometric datatypes. The mission design and navigation to enable repeat-pass interferometry at Venus are described.

INTRODUCTION

A deep understanding of solar system evolution and a better understanding of exoplanet habitability is hampered by the unanswered question: Why are Earth and Venus so different? We know that these twin planets formed with similar bulk composition and size. Yet Venus followed a divergent evolutionary path, losing its surface water and becoming hotter than Mercury. How did this happen? The answer has profound implications for the potential for life in the universe and how terrestrial planets become habitable.

Repeat-pass interferometry (RPI) is a powerful radar technique that can detect changes in the topography of a surface with sub-wavelength precision. These topographic changes can be driven by active magmatic and tectonic processes. Synthetic aperture radars onboard aircraft have detected ground motion on the scales of a few millimeters. To perform RPI, the radar must repeat its path over the topography of interest to within a fraction of the critical baseline length. This critical length defines a “tube” through which the spacecraft must fly.

REPEAT PASS INTERFEROMETRY

Differential radar interferometry¹ is routinely used to measure millimeter-level surface deformation by acquiring radar observations on temporally separated images spanning a time interval over which the surface was deforming. The vector separating the two platform positions when a

^{*} Mission Design Engineer, M/S 264-850

[†] Mission Design Engineer, M/S 301-121

[‡] Navigation Engineer, M/S 264-339

[§] Navigation Engineer, M/S 264-282

^{**} Senior Research Scientist, M/S 300-235

Jet Propulsion Laboratory, California Institute of Technology, Pasadena, CA 91109

point is imaged is called the baseline vector and the parallel and perpendicular components of the baseline are the projections onto the radar line-of-sight and cross line-of-sight (in blue) directions as shown in Figure 1.

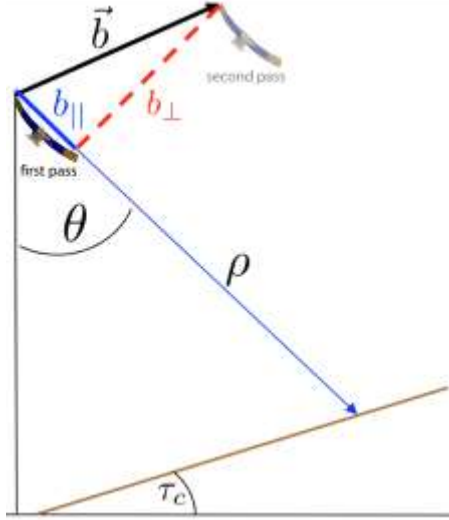


Figure 1: Parallel and perpendicular components of the interferometric baseline

Viable repeat pass interferometry is only possible when the perpendicular component of the baseline is less than the critical baseline, b_c , given by:

$$b_c = \frac{\lambda \rho \tan(\theta - \tau_c)}{2\Delta\rho} \quad (1)$$

where λ is the radar wavelength, ρ is the range, θ is the look angle, τ_c is the cross-track slope and $\Delta\rho$ is the range resolution of the radar. The critical baseline corresponds to when the geometric correlation, γ_g , given by:

$$\gamma_g = 1 - \frac{b_\perp}{b_c} = 1 - \frac{2b_\perp \Delta\rho}{\lambda \rho \tan(\theta - \tau_c)} \quad (2)$$

becomes zero. We set our minimal allowed geometric correlation to 0.8 to provide for robust repeat pass radar interferometric measurements yielding a maximum tube diameter of 160 meters.

MISSION DESIGN

Three perturbations, drag, eccentricity vector evolution due to the non-spherical Venus gravity field, and inclination torquing due to solar tides drive a Venus orbiter's trajectory away from the Keplerian ideal and an exact repeat. These perturbations must all be considered in the design of the operational orbit and in targeting and navigating to the tube. The design considered here is a representative² near-circular, near-polar orbit: 179×255 km altitude at 88.5 deg inclination. The perturbations need not necessarily be cancelled in their entirety, but need only be sufficiently cancelled to fly through the tube while the RPI measurements are being taken.

In order to do the interferometry, a full radar dataset must be returned to Earth. The quantity of data and the realities of link budgets across interplanetary distances mean that RPI cannot be done globally. As a result, we consider here "postage-stamp" or "targeted" RPI, where the measurements

are taken for 30 seconds an orbit over 20 consecutive orbits so as to observe a patch of ground roughly 200 km square. This is the equivalent of looking at Southern California from Santa Barbara to northern San Diego or the San Francisco Bay Area from San Jose to Sacramento and inland to the foothills of the Sierra Nevada.

Atmospheric Drag

The first perturbation is drag, which has been studied at length. The effect of drag is to reduce the semi-major axis of the orbit. For a sufficiently eccentric orbit, it also reduces the eccentricity by lowering apoapsis preferentially. This has two effects on targeting the tube. The altitude change is the first, and obvious, effect. The second is a cross-track effect. If the orbit is lower than the reference, the ground-track will drift to the east. If higher, it will drift west³. This leads to the classic “horseshoe” maintenance sequence⁴ where the orbit starts above and to the east of the reference altitude and track. Atmospheric drag is then permitted to lower the orbit as it drifts toward the track. Ideally, when the orbit is at the reference altitude, the ground-track has drifted to the edge of its tolerance and the track drift reverses itself as drag continues to lower the orbit. A drag make-up maneuver (or DMU) then raises the orbit when either an altitude or maximum ground-track offset is reached. The initial offsets are typically set such that a lower-than expected drag would still meet the western edge of the ground-track limit, as shown in Figure 2.

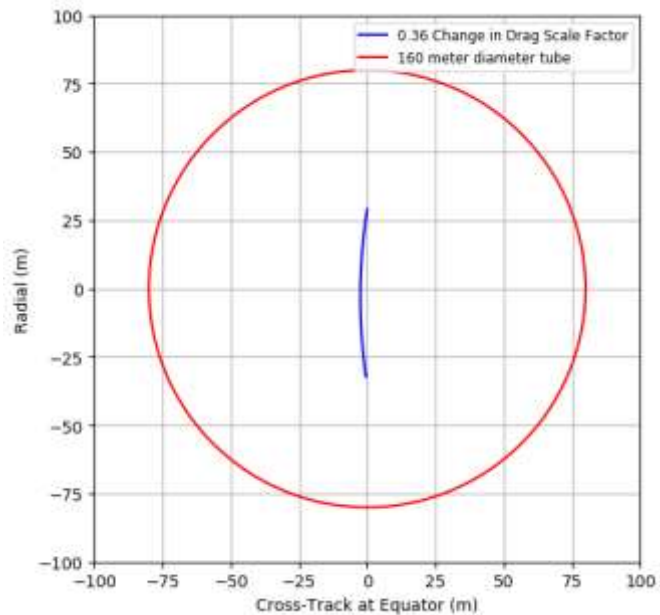
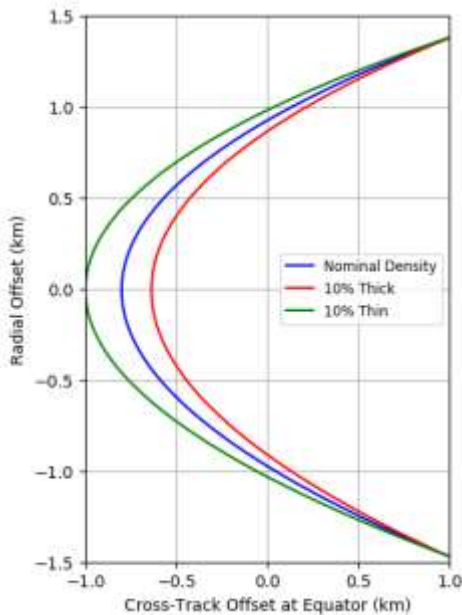


Figure 2: Horseshoe Ground-Track Maintenance **Figure 3: 99th Percentile Effect of Drag Uncertainty**

For the repeat pass interferometry requirement of flying through a 160 meter diameter tube laid down by a previous overflight, the same kind of horseshoe applies. However, the reference is not an absolute altitude and ground-track as in traditional orbit maintenance, but instead what was laid down by the previous trajectory. If the second overflight targets the same altitude and ground-track as was experienced by the first overflight, then the only drag-induced trajectory difference would be due to changes in the atmospheric density over the intervening time. Drag variation is typically parameterized as a scale factor on the atmospheric density model. This covers not just actual density variation but also cross-sectional area, coefficient of drag, and other effects. The 99th percentile of variation from one pass to the next is a 0.36 change in scale factor if we conservatively assume that

0.1 is the standard deviation of the scale factor. For an example 218 km circular orbit, a reasonable area/mass ratio, and a scale factor change from 0.829 to 1.197, the second pass will drop 62 meters more than the first pass did in 20 orbits, if the change is compensated for in the targeting, as illustrated in Figure 3. Without compensation, the drop is closer to 72 meters, and the crosstrack difference would grow from 2.3 to 11 meters.

Operationally, the flight team will need to reconstruct and trend the drag scale factors to account for this predominately-radial motion in the tube. If the atmosphere is predicted to be thicker than was experienced in the previous baseline, the trajectory will need to be adjusted to a higher initial condition. The reverse is true if the drag is predicted to be less. The reference altitude will drop faster than the second pass, and so the spacecraft will appear to rise relative to the tube center. Managing the ground-track motion here is far simpler. In both cases, the ground-track will shift a few meters from the reference and need not be specially compensated for, if the altitude is properly compensated. Maintaining the orbit such that the ground-track offset is aimed to be zero at the targeted sites would be an ongoing process.

Venus Non-Spherical Gravity

The second perturbation is due to Venus’s extraordinarily slow 243-day sidereal period. The ground-track at the equator only moves about 10 km per orbit. As a result, the same gravity perturbations are experienced repeatedly on subsequent orbits. This drives significant inclination and eccentricity vector evolutions. The inclination varies by ± 0.5 deg but essentially repeats (see Figures 4 and 5). However, the eccentricity vector sees a secular shift and the altitude vs. ground-track position would be radically different (see Figure 6). A similar effect is experienced by lunar orbiters⁵. The primary effect of this eccentricity vector shift is to force the design away from a circular orbit. To maintain the orbit to within 80 meters of circular would require an eccentricity reset maneuver every few hours. By allowing the orbit to evolve over the course of a ground-track repeat cycle and then resetting at the end of the cycle (or at pre-determined times within a cycle), the operational tempo can be more reasonable. In order to ensure that the spacecraft flies within the tube on subsequent passes, this eccentricity vector evolution must be reset to follow the same path every cycle.

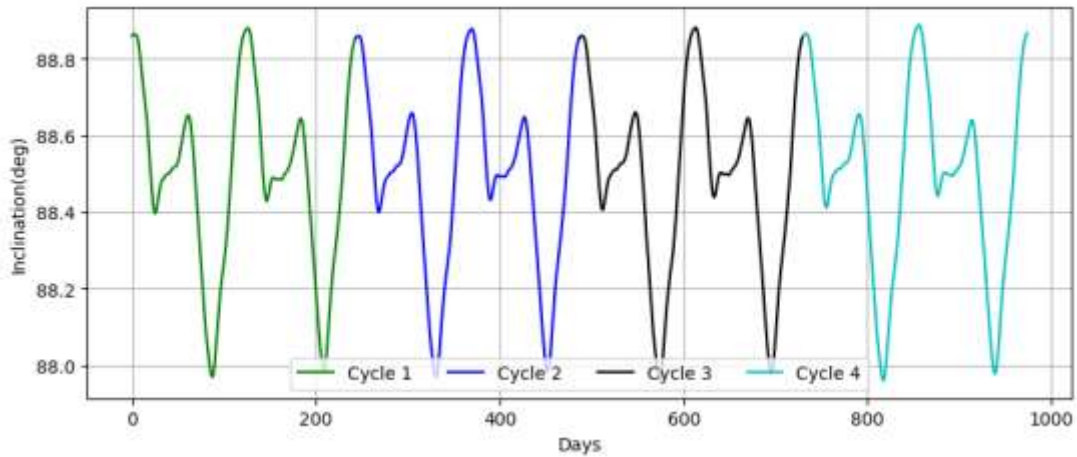


Figure 4: Inclination variation over four ground-track repeat cycles

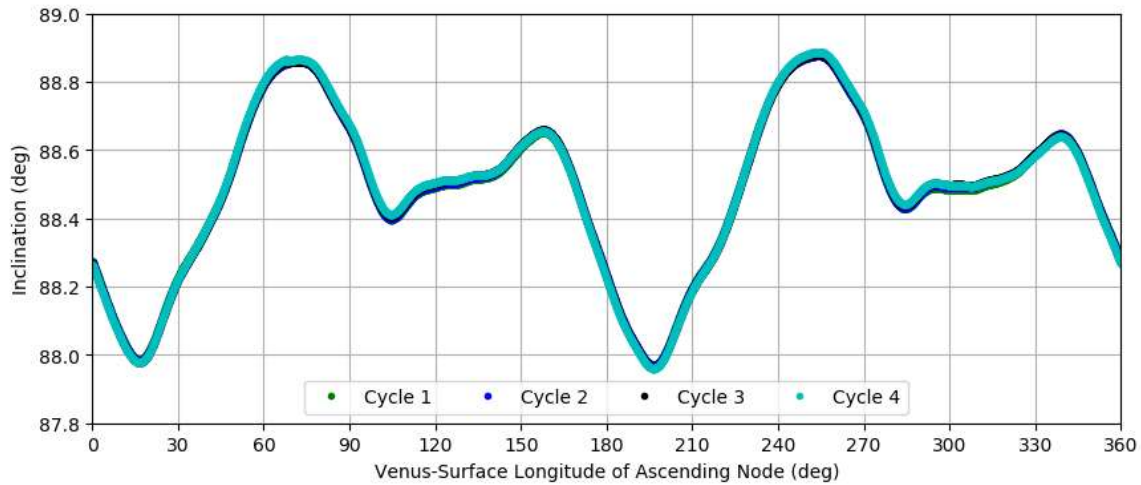


Figure 5: Inclination variation is dominated by Venus non-spherical gravity

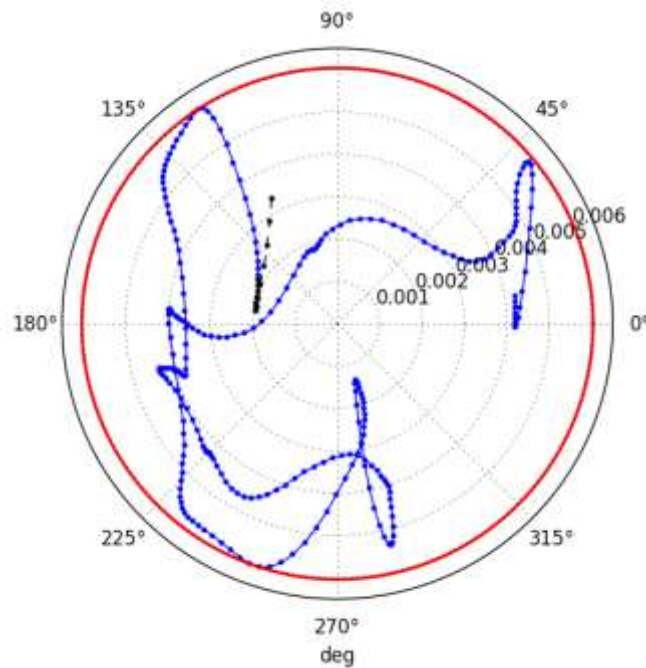


Figure 6: Eccentricity Evolution of a low Venus Orbiter. The first 10 days (black) of one Cycle are not identical to the first 10 days (upper right, in blue) of the following Cycle.

Both of these effects are deterministic (unlike drag) and repeat exactly with the topography (unlike solar torques), and so do not contribute to relative motion of the tube, except inasmuch as execution errors in the eccentricity vector resets require clean-up. However, it has been shown⁶ that an initial small offset in eccentricity and argument of periapsis ($e-\omega$) space (as in Figure 6) of the eccentricity vector remains nearly constant over time. That is, the $e-\omega$ state transition matrix is effectively identity, and residual errors due to clean-ups can be made nearly arbitrarily small if sufficient maneuvers are planned. Small variations in inclination and the ascending node remain similarly small after a 243.3-day ground-track repeat cycle, illustrated in Figure 7. Note that the inclination at the end of a cycle is the same as at the start, but the ascending node has shifted slightly

more than 0.4 degrees. This is the extraordinarily slow precession of the ascending node due to a J_2 three order of magnitude smaller than Earth's and is why the repeat cycle is 0.3 days longer than the sidereal day.

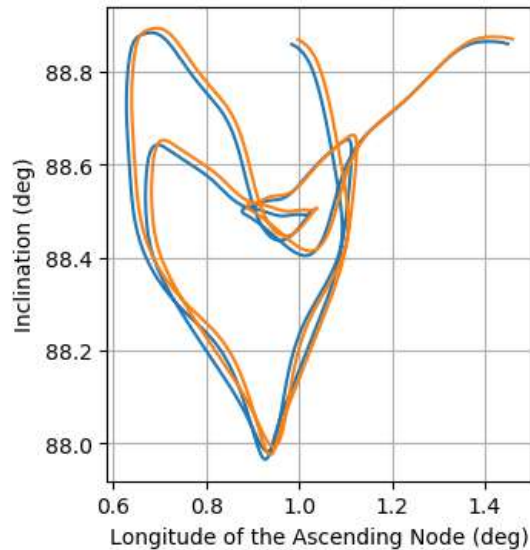


Figure 7: Small variations in inclination and ascending node remain small.

Solar Torques

The third effect is solar torquing of the orbit plane. If Venus were tidally locked, this would not be an issue, as the solar effect would repeat along with the non-solar gravity effect. However, Venus is not tidally locked; its orbit period is 224 days. The solar perturbation on inclination, averaged over an orbit, is given by:

$$\left. \frac{di}{dt} \right|_{AV} = -\frac{3\mu_s}{2r_s^3} \sqrt{\frac{a^3}{\mu}} \sin i \sin(\lambda - \Omega) \cos(\lambda - \Omega) \quad (3)$$

where μ_s and μ are the gravitational parameters of the sun and Venus, respectively, r_s is the range to the sun, a is the orbit semi-major axis, i is the inclination relative to Venus orbital plane, λ is the longitude of the sun, and Ω is the orbital ascending node. Venus is in a very nearly circular 0.718×0.728 AU orbit with an orbit obliquity of 2.6 deg. From perihelion to aphelion, a low Venus orbiter would only experience a 4% change in this rate. A polar orbit would experience an even smaller rate change due to the obliquity: 0.1%. For conservatism, we shall assume the maximum rate for our 179×255 km orbit of 4×10^{-9} deg/sec (including the sine and cosine terms at their maximum value of 0.5). At maximum latitude, this corresponds to 48 meters of total cross-track motion over 20 orbits. Assuming an 88.5 deg inclination orbit, this is reduced to 42 meters at 60 deg latitude. It is a mere 24 meters at 30 deg latitude. Three ground-track repeat cycles into the mission, the inclination change due to solar torque is almost 180 degrees out of phase from the first cycle, as illustrated Figure 8.

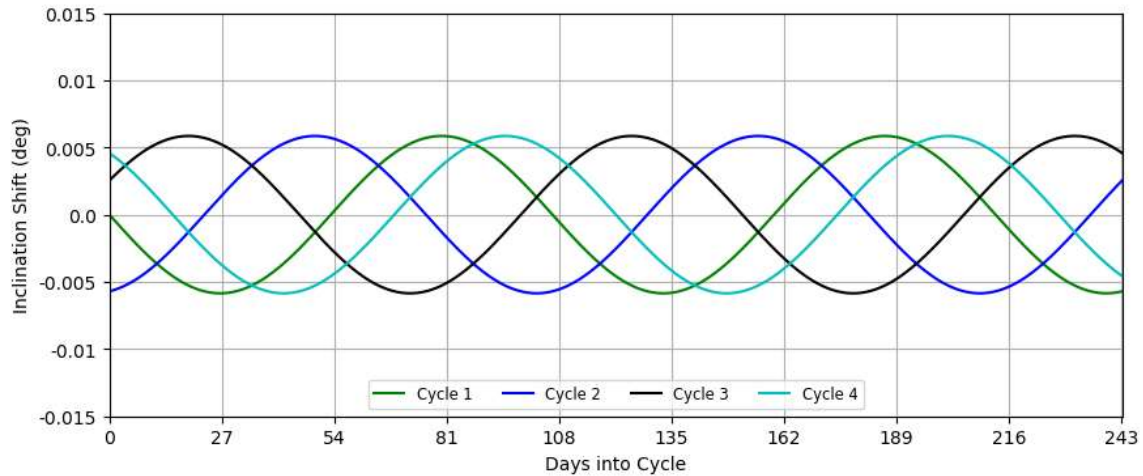


Figure 8: Inclination variation due to solar torque over four ground-track repeat cycles

This ± 0.006 deg variation in inclination results in a ± 682 meter crosstrack variation at maximum latitude, far in excess of the ± 80 meters permissible within the tube, and so this effect must be managed. The operationally simplest way to manage the inclination is to target back to the perturbed inclination of the first observation. That is, make an initial observation of the target in Cycle 1 and then crank the orbit up or down to that inclination in each subsequent cycle. The problem with this approach is that in Cycle 3, the relative inclination rates have almost doubled (see Figure 9), to 7.8×10^{-9} deg/sec, which leads to 94 meters of relative motion. While 94 meters is sufficient to remain in a 160-meter tube with appropriate targeting, it reduces the allowable uncertainty in navigating to the tube entrance. While it costs slightly more propellant to target each observation to an idealized “no-sun” reference as in Figure 8, since doing so requires a maneuver for every target, the reduction in relative tube motion is worth the expense, since a worst-case inclination adjustment is only 0.75 m/s to correct a 0.006 deg offset. The average cost is far less, 0.55 m/s.

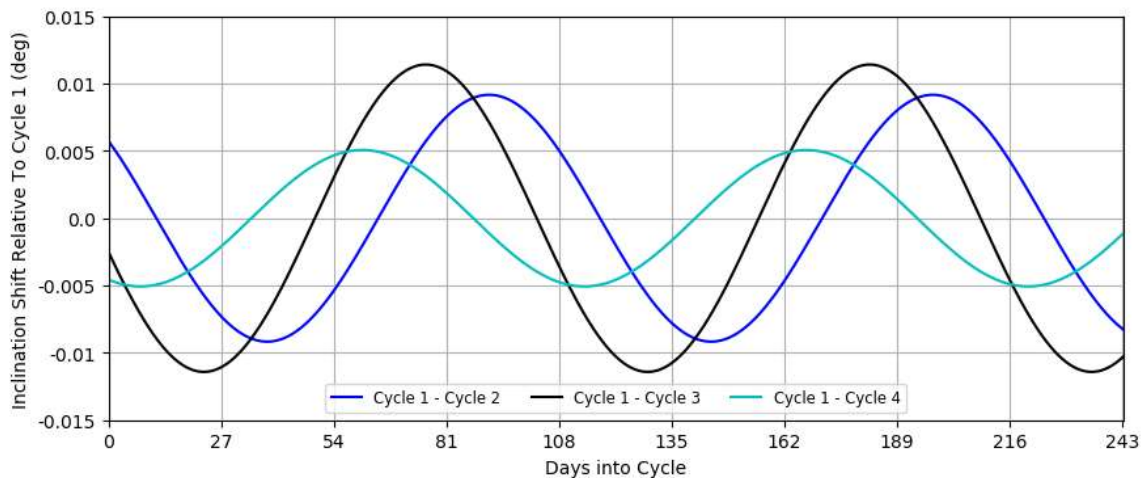


Figure 9: Inclination variation due to solar torques relative to a previous cycle.

NAVIGATION

In general, two-way X-band range-rate tracking data is sufficient for navigation at Venus. However, geometric special conditions arise frequently enough that a combination of two-way Doppler

and two-way-minus-three-way Doppler is a preferable base-line tracking plan. Two-way-minus-three-way Doppler is valuable because it provides a plane-of-sky velocity component – important for reducing cross-track axis error. For brevity, two-way-minus-three-way Doppler will henceforth be referred to as differenced Doppler. Additionally, if the telecommunication subsystem can provide Ka-band downlink, Ka-band tracking data can be base-lined as well. Ka-band adds margin to navigation solutions at Venus, especially for the worst-case geometric condition of an edge-on orbit plane during conjunction.

Daily requirements for navigation are driven by the surface elevation mapping campaign. A successful campaign depends upon on-board processing of the surface measurements – for which an on-board, *predictive* ephemeris is needed. The on-board ephemeris is valid for two to three days and is generated daily from navigation solutions. RPI science requirements, on the other hand, are more stringent in predictive ephemeris with respect to the Venus surface for targeting the tube entry and are driven by ephemeris *reconstruction* accuracy. For the spacecraft to follow a Venus-relative trajectory laid down by earlier orbits over the same site, controllers must be prepared to position two (non-consecutive) orbit paths within 160 m of each other along path at least 200 km in length. Inclination errors, eccentricity errors, orbit-torquing errors, and maneuver execution errors all contribute to missing the tube. Since Venus’s rotation period is uncertain, it too is an error contributor, varying by up to ± 5 min over decades⁷ and perhaps by ± 1 min over one month⁸.

Orbit *reconstruction* of RPI passages can have high fidelity if terrain-relative, radar tie-point data are incorporated to determine the Venus-relative position of the spacecraft (see Table 1). Tie-points are empowering in this application, as discussed in the following section.

Reconstruction via Radar-Based Terrain-Relative Navigation

The navigation subsystem can supplement Doppler measurements with radar tie-point observations⁹ to compensate for Venus’ rotation uncertainty. A radar tie point is the identification of the same surface feature in two or more radar images. Tie points are used to build a frame-tie, relating the J2000 frame to the Venus Body Fixed frame. This precise knitting-together of coordinate frames enables RPI science observations.

Radar tie-point observables are range and relative-velocity between the orbiter and the landmark. They are defined by a set of seven data elements, each set specific to a particular orbit and radar swath. See the Appendix for a description.

For RPI reconstruction, terrain-relative observations and two-way Doppler measurements are sufficient to meet science goals. Differenced-Doppler is unnecessary. Thus, two-way X/Ka Doppler combined with terrain-relative measurements satisfy science goals. (Differenced-Doppler is needed for some predictive ephemerides but not for reconstructed ephemerides.) This offers more flexibility for DSN schedulers, as the contingency of planning for station view-period overlaps is eliminated.

We note that the value of terrain-relative observations for orbit determination strengthens as more tie-points are acquired. Fewer than 10 tie-points connecting orbits i and j are ineffective; we suggest a bare minimum of 20 for any pair of orbits. In this preliminary analysis, we simulated 49 tie-points. Reconstructions are even more robust when hundreds of tie-points are identified.

To simulate tie-point observables for this analysis, two spacecraft trajectories were generated: a nominal ephemeris and a $1-\sigma$ perturbed ephemeris. The difference in platform position between orbits i and j then defines the $1-\sigma$ offset between subsequent images of each tie-point. The offset represents our expectation of the actual conditions during data-taking – slightly different observed

locations of the same tie-point on subsequent orbits. The best estimate of the tie-point’s true coordinates is determined by a least-squares fit of multiple views of the same point.

Results from our first attempt at incorporating simulated Venus-centered landmark data into a solution are shown in Figure 10. We used 49 tie-point landmarks acquired over 15 hours (~9 orbits). Landmark locations were determined using a least-squares fit of those observations. The left figure represents range residuals – the distance from the orbiter to the landmark. The right figure represents range-rate residuals – the velocity of the orbiter with respect to the landmark.

The fits are flat, indicating the simulated data, the dynamic models, and the landmark locations are in rough agreement (subject to loose tolerances). The mean in Figure 10-left is 6 m +/- 1.9 km and Figure 10-right’s mean is 1.7 m/s +/- 150 m/s. While the scatter around these averages is large, the statistics are tolerable in light of the tie-point simulation procedure. It is a laborious, multi-step, hands-on process subject to a lot of (subtle) rounding error. The 49 tie-point data set is also *de minimus*. However now that a simulation methodology has been established, in future analyses the procedure can be automated, thereby minimizing systematic errors and simplifying the generation of numerous tie-points.

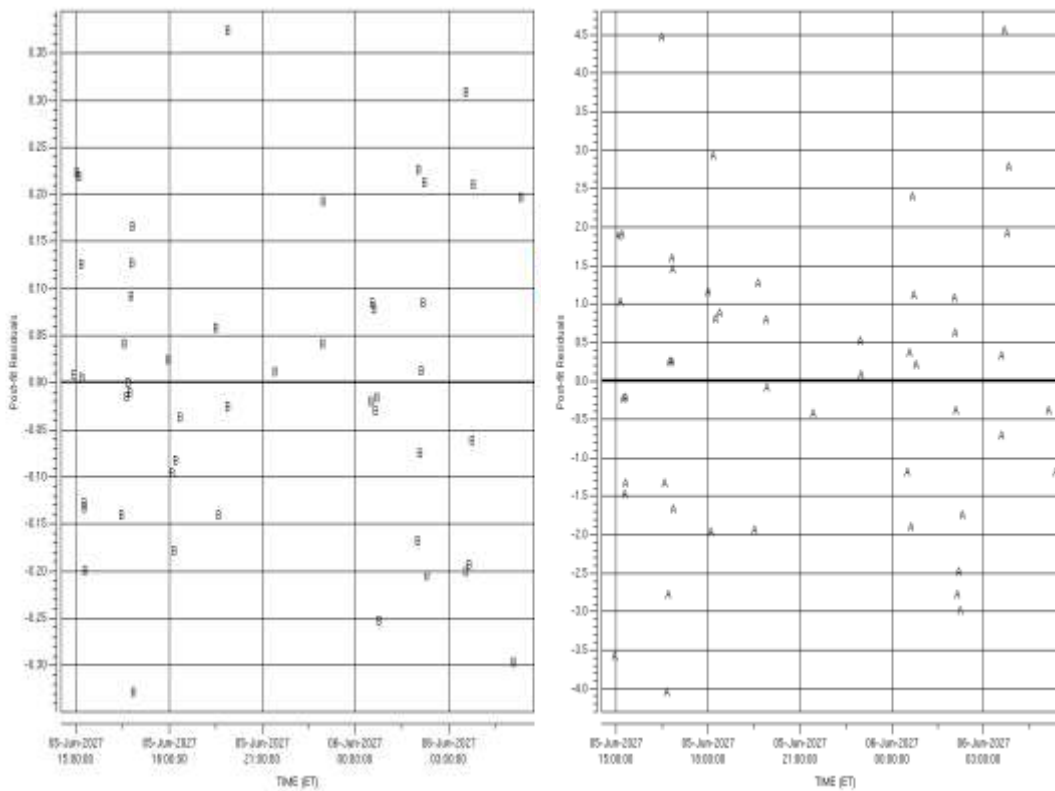


Figure 10: Position (left) and Velocity (right) tie-point residuals for a face-on geometry

Combining two-way tracking with terrain-relative measurements reduces cross-track uncertainty significantly with respect to radiometric-only solutions – especially for an edge-on configuration. The cross-track error for face-on orbit geometry shrinks from $\sim\pm 100$ m to $\sim\pm 10$ cm, while the cross-track error for an edge-on orbit geometry is reduced to ± 5 meters. See Table 1 and Figure

11

Table 1: Orbit Reconstruction Capability (9 hours/day X/Ka Doppler, 2-day data arc)

Component	Knowledge with Tie-points (3σ)
Radial position (m)	$\pm 0.1^{EO}$
Along-track position (m)	$\pm 10^{FO}$
Cross-track position (m)	$\pm 15^{EO}$

FO – worst case is face-on orbital geometry EO – worst case is edge-on orbital geometry

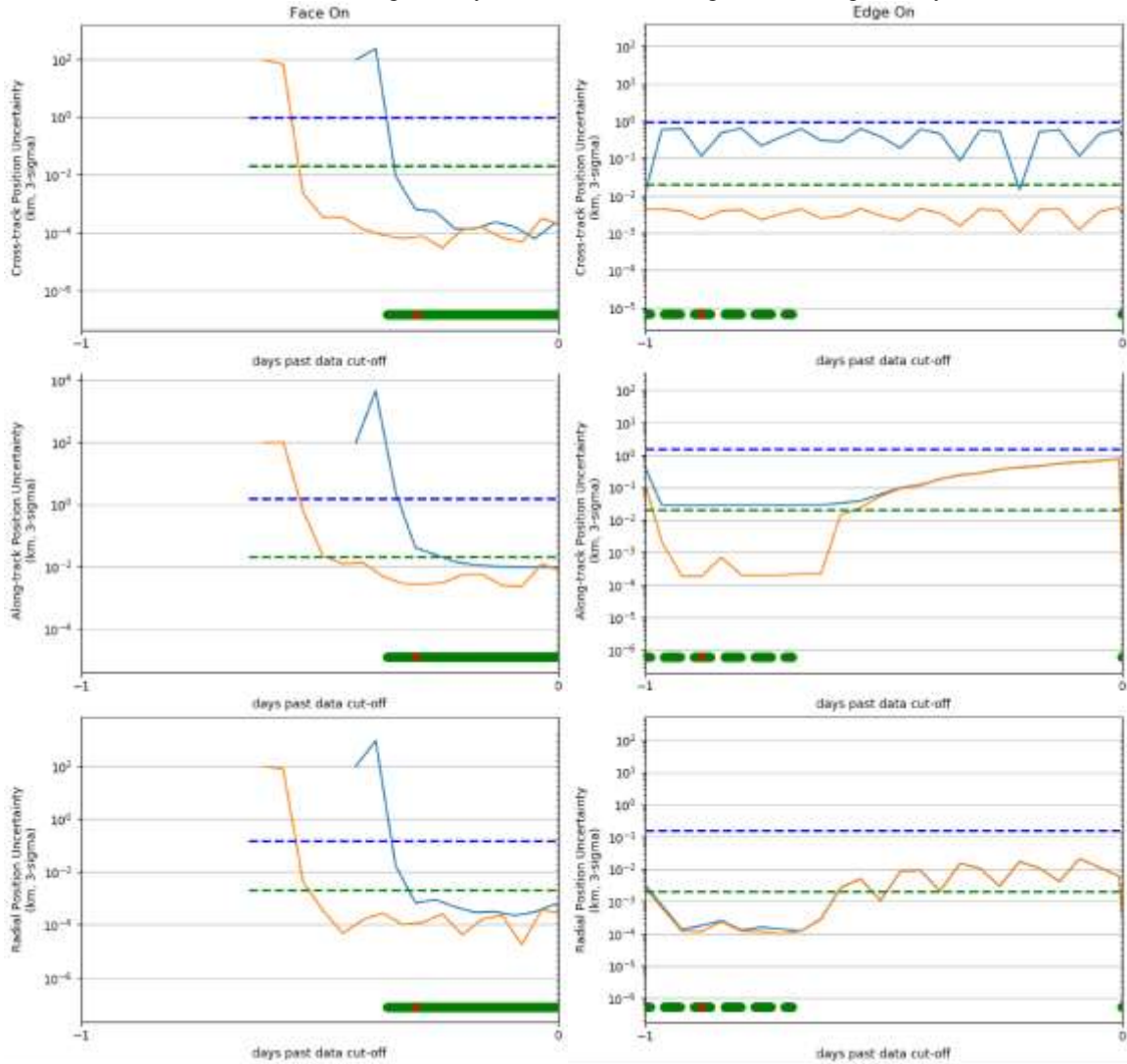


Figure 11: Reconstructed position knowledge for a face-on (left) and edge-on (right) geometries using Doppler tracking only (blue) and with radar tie-points (orange), compared to initial and final radar processing requirements (blue and green dashed lines, respectively)

Table 4 in the Appendix lists modelled error sources for the orbit reconstruction analyses.

Spacecraft Prediction via Doppler and Ranging

Commanding the spacecraft to thread the tube, once it is known sufficiently well, can be accomplished using the baseline data set of tracking data for certain geometries. The worst-case geometry is one such that the orbit plane is edge-on to the Earth. In this geometry, the cross-track uncertainty maps into the plane of the sky and is difficult to observe. With a two-day advance notice prior to tube-entry, the predicted ephemeris cross-track error at tube entry can be as large as ± 126 m (3σ) from the target, with components at 60 deg latitude detailed in Table 2 [Error! Reference source not found.](#) The budget is dominated by the ± 120 m error in the orbit plane at the tube entrance. In the best-case, face-on geometry, this error is reduced to ± 20 m (see

Table 3). The other components of the budget are insensitive to this geometry change, so the total cross-track error is reduced to ± 45 m (3σ). Some components are sensitive to latitude, however. The Venus rotation period uncertainty grows from ± 5 m to ± 20 m between the equator and 60 deg latitude, but the execution errors in the inclination adjustment maneuvers have nearly the exact opposite trend, going from ± 20 m to effectively ± 0 m. The total budget, then, is insensitive to latitude, but sensitive to the Earth beta angle. These estimates include the traditional and generous margins on the navigation inputs, such as measurement noise and dynamical errors. They also include 100% margin on the reconstruction results above.

The radial uncertainty, also detailed in

Table 3, varies with the Earth geometry as well, but not nearly so dramatically.

Table 2: Cross-Track Error Budget at 60 deg Lat

Cross-Track Error Budget for Repeat-Pass Interferometry	Worst-Case, Edge-on Geometry (m, 3σ)	Best-Case, Face-on Geometry (m, 3σ)
Error in knowledge of first-pass orbit in space		
Error in first-pass orbit position with respect to Venus features	± 20	± 20
Error in Venus feature positions on Venus rotation model	± 20	± 20
Error in Venus rotation model prediction of Venus rotation	± 13	± 13
Error in control of second-pass orbit position in space		
Error in orbit plane prediction at RPI tube entrance	± 120	± 20
Error in Venus rotation from timing of spacecraft arrival at tube	± 13	± 13
Error in position from final targeting maneuver execution	± 20	± 20
Total (RSS)	± 126	± 45

Table 3: Spacecraft Position Uncertainty at RPI Tube Entrance

Earth Geometry (Earth Beta Angle)	Cross-Track (m, 3σ)	Radial (m, 3σ)
0 deg (Edge-On)	± 120	± 60
20 deg	± 110	± 55
55 deg	± 70	± 20
90 deg (Face-On)	± 20	± 26

SITE TARGETING

In order to accomplish repeat pass interferometry, each 200×200 km surface target must be identified in advance. The ground-track walk would need to be managed continuously such that the offset from the ground-track reference at the target is zero, as in Figure 2. This continuous management would take place within the context of a larger ground-track tolerance set by instrument swath overlap and other, non-RPI considerations. A week prior to the overflight, an inclination adjustment maneuver would be performed to center the projected inclination variation from a no-sun reference, as in Figure 8, on 0 deg variation. Two days prior to the overflight a final maneuver would be performed to achieve the radial target offset by the predicted difference in drag as in Figure 3. Each of these maneuvers can include a component to clean up the execution errors in the previous maneuver(s). For the first overflight, the radial component target would be relative to a mean drag prediction. For subsequent overflights of the surface target, the tube entrance target is thus not the center of the tube as defined by the initial overflight. It is offset in both radial and cross-track by the predicted drag and inclination-rate differences, respectively.

The probability of successfully entering the RPI tube is a function of this target offset and the delivery uncertainty discussed in the previous section. An example at 60 deg latitude is illustrated in Figure 12, where the differential drag prediction is at the 99th percentile, causing a 62 meter radial offset, and the inclination rates are at their maximum, causing a 42 meter offset in the cross-track motion. Combined with the 3σ 62.8×22.5 m delivery error corresponding to an Earth beta angle of 70 deg, there is a 99.3% chance of successfully navigating to the tube entrance and remaining in the tube for all 20 desired orbits.

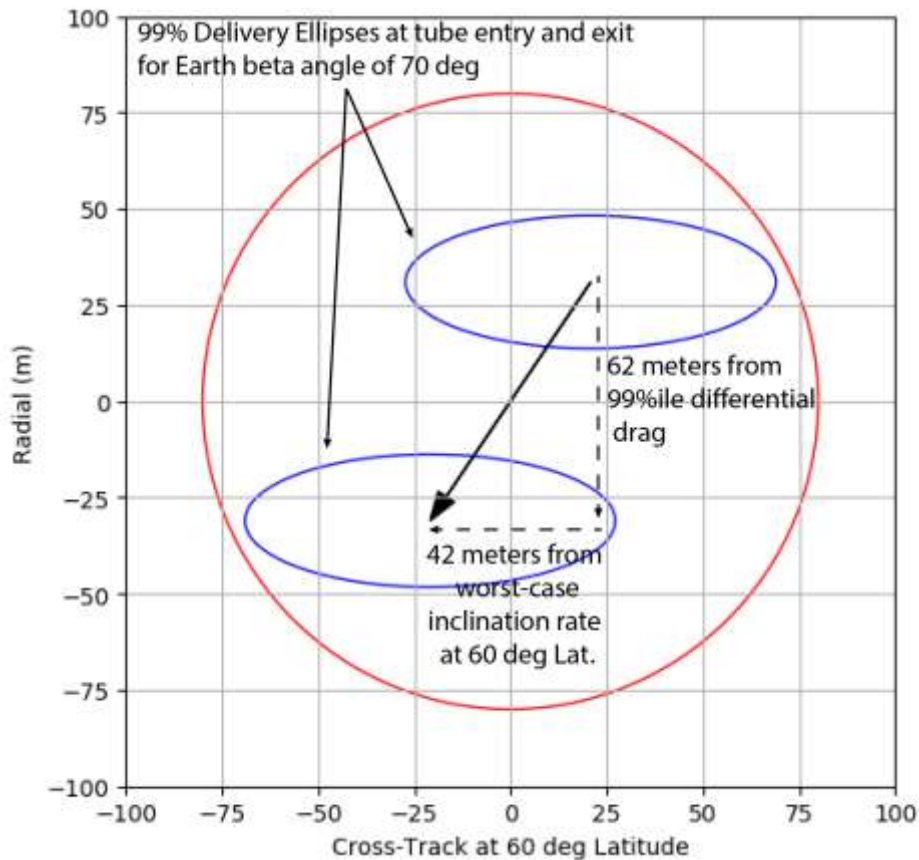


Figure 12: Worst-on-Worst relative tube motion (arrow) meets the 160-m RPI tube (red) with better than 99% delivery (blue) for an example Earth geometry

By varying the necessary cross-track offset target with the local solar time of the orbit and applying the delivery uncertainty as a function of the Earth beta angle, a contour plot of the probability of successfully entering a tube at a given latitude can be generated as in Figure 13 for 60 deg. As can be seen in Figure 13, the minimum probability is approximately 85%, corresponding to the worst-on-worst-on-worst case scenario of the 99th percentile change in the drag, the worst-case inclination rates, and the worst-case delivery uncertainty in the edge-on-to-Earth geometry applied to a relatively high-latitude target. The probability increases to over 99% (highlighted in green) when the spacecraft orbit is within 24 to 39 deg of face-on to the Earth, depending on the inclination rates, which have less of an impact at lower latitudes. The yellow region corresponds to those geometries with a 90-99% probability of success. In this region, two attempts have a 99% chance of at least one success. For an example mission profile, illustrated in Figure 13, 89% of the Venus surface above 60 deg latitude has at least one overflight after the first ground-track repeat cycle when the geometries are most favorable. The remaining 11% of the surface has at least two overflight opportunities with a greater than 90% chance of success. As a result, with careful scheduling, the entire surface of Venus could be available for RPI.

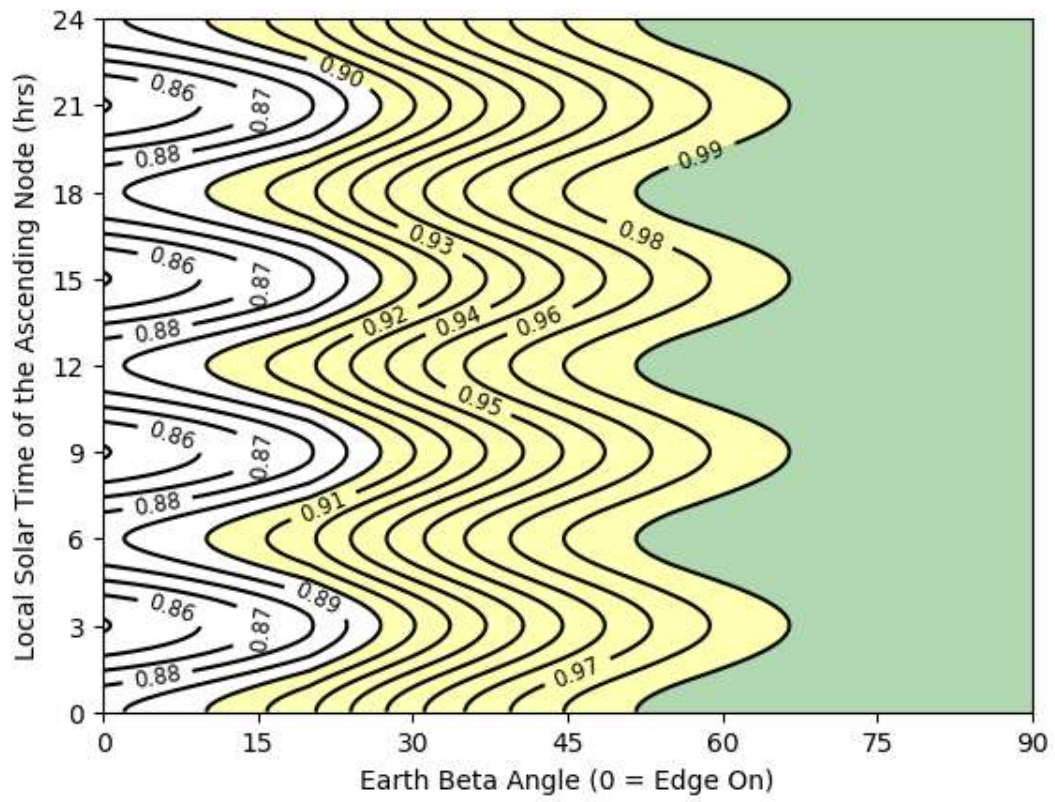


Figure 13: Probability of Successfully Entering an RPI Tube at 60 deg Latitude

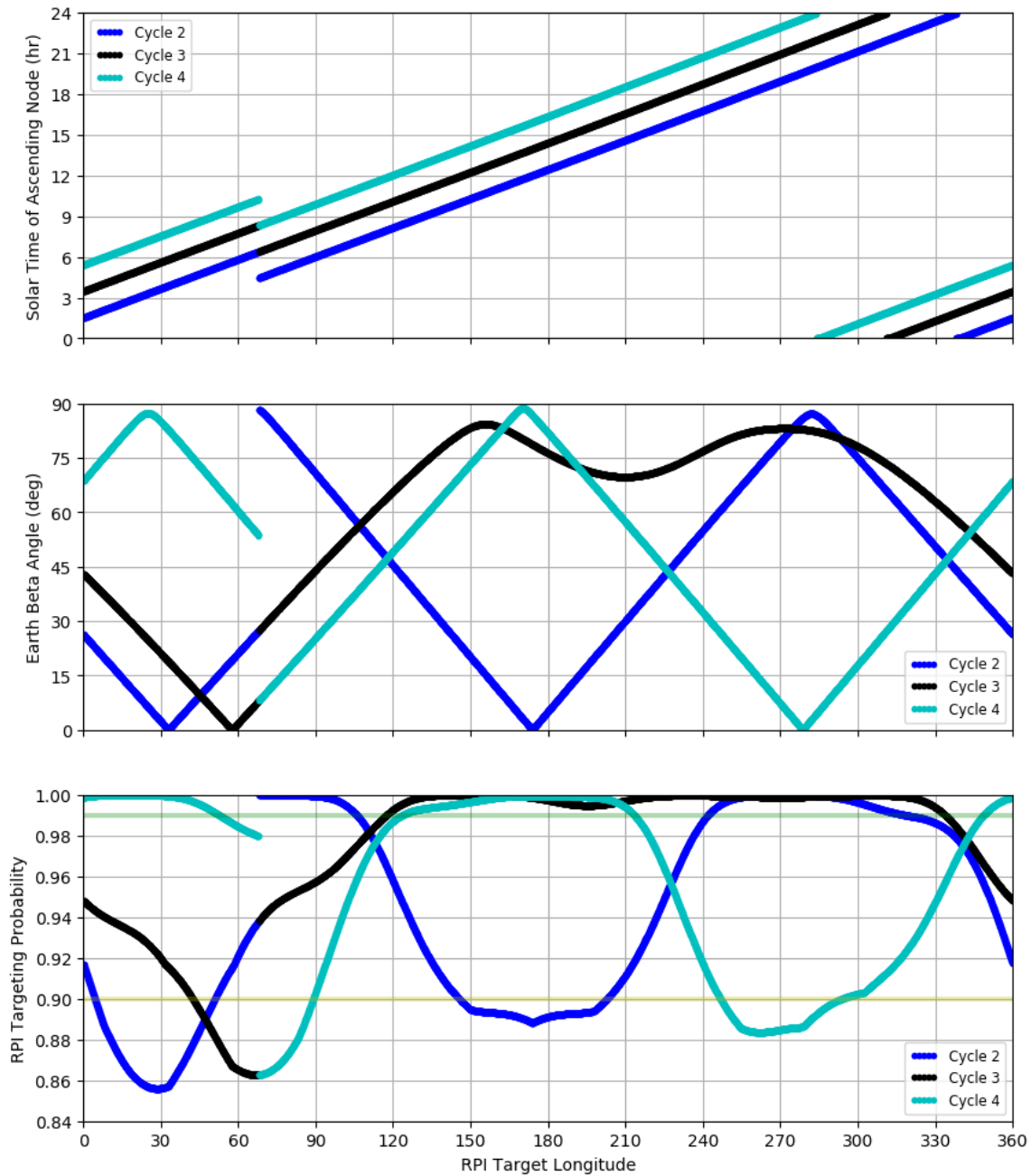


Figure 14: Combining the inclination rates (driven by the solar geometry, top) and the delivery error to the tube entrance (driven by the Earth geometry, middle) yields a probability of successfully entering a tube at 60 deg latitude and various longitudes (bottom) for an example mission profile.

CONCLUSION

Repeat pass interferometry is a supremely powerful technique for determining current geologic activity, from the motion of magma chambers deep underground to surface deformations due to earthquakes. It has been used to study these phenomena here on Earth and we can do so at Earth's

twin, Venus. By using the enabling technique of radar tie points to knit together the inertial and geocentric coordinate frames of radio-based navigation to the surface of Venus, we can exquisitely reconstruct where the spacecraft previously over-flew the region of interest. This has the by-product of generating a Venus rotation model with an order of magnitude better orientation accuracy than is currently available. Then, using the traditional navigation techniques of Doppler and ranging, we can target the spacecraft to fly within 80 meters of that previous track with 99% reliability when the geometries are favorable and enable this potentially transformational scientific measurement.

ACKNOWLEDGMENTS

This work was performed at the Jet Propulsion Laboratory, California Institute of Technology, Pasadena, California, under contract to the National Aeronautics and Space Administration.

APPENDIX: RADAR TIE POINTS

Radar tie points consist of the following information, where i and j denote orbit numbers for two radar swaths, each of which view the same surface feature:

- The times, t_j and t_i , when a given feature (or tie point) is imaged by the orbiter on orbits i and j , respectively.
- The Venus Body Fixed positions of the orbiter, $\sim P_i$ and $\sim P_j$ when the tie point is imaged on orbits i and j .
- The Venus Body Fixed velocities of the orbiter, $\sim V_i$ and $\sim V_j$ when the tie point is imaged on orbits i and j .
- The *a priori* Venus Body Fixed coordinates of the tie point, $\sim T_i$ and $\sim T_j$.
- The ranges r_i and r_j when the tie point is imaged on orbits i and j .
- The Doppler frequencies f_i and f_j when tie point is imaged on orbits i and j .
- A range-frequency error covariance matrix, C_{ij} , of the form

$$C_{ij} = \begin{bmatrix} \sigma_r^2 & \sigma_{rf}^2 \\ \sigma_{fr}^2 & \sigma_f^2 \end{bmatrix} \quad (4)$$

Table 4: Reconstruction Error Sources

Error Source	Error (1σ)	Comments
Orbiter <i>a priori</i> state	30 km (spherical) 100 m/s (spherical)	Wide open initial state.
Landmark location - latitude & longitude	0.5 deg	Notable surface landmarks selected to become radar tie points.
Gravity field (15x15)	MGNP120	GM & covariance from Magellan.
Momentum desaturation im- pulses	0.6 mm/s (spherical)	Performed once per day.
Tube-targeting ΔV	1.0 cm/s (spherical)	Not part of RPI reconstruction
Tube-targeting cleanup ΔV	5.0 mm/s (spherical)	Not part of RPI reconstruction
Atmosphere density	10%	VenusGRAM2005 atmosphere. Scale factor estimated stochastically.

Error Source	Error (1σ)	Comments
		White noise, 8-hour batch.
Solar radiation pressure	5%	Scale factor
UT1, Earth pole (X,Y)	21 us, 43 ndeg	Considered
Media (trop & ion)	Standard error	Considered
DSN station locations	Standard cov.	Considered
Data Type	Measurement error (1σ)	Comments
X/Ka 2-way doppler	4 mhz	= 0.07 mm/s
X/Ka differenced-doppler	3 mhz	= 0.05 mm/s. Scheduled within $\pm 30^\circ$ of edge-on orbit geometry
Tie point measurement	1 cm, 50 cm/s	Relative position & velocity of landmark with respect to orbiter at time of radar observation.

REFERENCES

- ¹ Rosen, P.A., et al., “Synthetic aperture radar interferometry” ,*Proc. IEEE*, Vol. 88, No. 3, March 2000, 333–382
- ² Freeman, A., et al., “VERITAS: a Discovery-Class Venus Surface Geology and Geophysics Mission” IEEE Aerospace Conference, Big Sky, MT, March 5-12, 2016
- ³ Bhat, R.S., et al, “TOPEX/Poseidon Orbit Maintenance for the First Five Years” AAS 98-379 AAS/GSFC 13th International Symposium on Space Flight Mechanics, Greenbelt Maryland, May 11-15, 1998
- ⁴ Vincent, M. A. “The Mutual Interactions between Drag Make-up and Mean Local Time Maneuver Designs” AIAA/AAS Astrodynamics Specialist Conference, Honolulu, Hawaii, August 18-21, 2008.
- ⁵ Sweetser, T. H., et al. “Design of an Extended Mission for GRAIL.” AIAA/AAS Astrodynamics Specialist Conference, Minneapolis, Minnesota, August 13-16, 2012.
- ⁶ Wallace, M. S. et al., “Low Lunar Orbit Design via Graphical Manipulation of Eccentricity Vector Evolution,” AIAA/AAS Astrodynamics Specialist Conference, Minneapolis, Minnesota, August 13-16, 2012.
- ⁷ Mueller, N.T., et al. “Rotation period of Venus estimated from Venus Express VIRTIS images and Magellan altimetry”. *Icarus* 217, 474–483.doi:10.1016/j.icarus.2011.09.026, 2012
- ⁸ Cottureau, L., et al. “The various contributions in Venus rotation rate and LOD.” *Astronomy & Astrophysics* 531:A45, 1–10, doi:10.1051/0004-6361/201116606, 2011
- ⁹ Chodas, P.W., et al., “Magellan ephemeris improvement using synthetic aperture radar landmark measurements.” AAS/AIAA Astrodynamics Conference 1991, Vol. 76 of the *Advances in the Astronautical Sciences* series, 875–890, Univelt, Inc., San Diego, 1992.